

Direct Comparison of the B^{12} and N^{12} Beta Spectra*

NEEL W. GLASS AND ROBERT W. PETERSON

Los Alamos Scientific Laboratory, University of California, Los Alamos, New Mexico

(Received 26 November 1962)

An experimental direct comparison of the shapes of the B^{12} and N^{12} beta decay spectra was made as a test of the validity of the conserved vector current theory (CVCT). The comparison was made at corresponding momentum points normalized to the end-point momenta of the spectra using a 5-channel 180° magnetic spectrometer. The comparative shape factor was measured to have an energy dependence of $1.62 \pm 0.28\%$ per MeV, to be compared with a predicted value of $1.10 \pm 0.17\%$ per MeV on the basis of the CVCT. The measured end-point energy of the N^{12} ground-state spectrum is 16.384 ± 0.015 MeV. The comparison of the spectra also yielded a value of $2.2 \pm 0.6\%$ for the branching fraction of the N^{12} decay to the 7.6-MeV level of C^{12} , $0.85 \pm 0.6\%$ for the fraction to the 10.1-MeV level, and an indication of a branch to one or more levels around 12 MeV.

I. INTRODUCTION

THE conserved vector current theory (CVCT) was proposed by Feynman and Gell-Mann¹ to account for the near equality of the muon decay coupling constant and the vector part of the beta-decay coupling constant as determined from the O^{14} decay. According to this theory, the vector coupling is generated by the interaction of a conserved current with itself, and in analogy with electrodynamics, the vector coupling remains the same in the presence of strong interactions, just as the total electric charge remains the same.

Gell-Mann has shown² that the CVCT has specific observable consequences in beta decay that may serve to determine the correctness of this theory as distinguished from the usual Fermi theory. A consequence is an enhanced term in the beta vector interaction. The interference between this term and the axial-vector term for a $1^+ \rightarrow 0^+$, $\Delta T=1$ beta transition results in a deviation from the allowed Fermi shape. Gell-Mann chose the B^{12} beta decay to the C^{12} ground state and the corresponding N^{12} positron decay as the most promising case, and calculated the magnitude of the effect from the rate of the analogous $M1$ gamma transition³ from the 15.11-MeV level in C^{12} .

The calculated shape factor is $1 + (8/3)aE$ for the B^{12} ground state decay and $1 - (8/3)aE$ for the N^{12} decay if no electromagnetic or inner bremsstrahlung effects are considered. E is the beta-ray energy and a is calculated by Gell-Mann to be $2.3/M$ where M is the proton mass. The comparative deviation is calculated⁴ to be

$$S(E, B^{12})/S(E, N^{12}) = \text{const}[1 + (A + \delta A)E]f(E), \quad (1)$$

where $S(E, x)$ is the spectrum of each transition divided

by the corresponding allowed Fermi spectrum. The function $f(E)$ is the inner bremsstrahlung correction necessary because of the difference in end-point energy.^{4,5} The calculated value for A is $1.35 \pm 0.07\%$ per MeV,⁶ and δA is an electromagnetic correction of $-0.25 \pm 0.15\%$ per MeV.⁴ If the CVCT is not assumed, the equivalent value of $A + \delta A$ is estimated to be about 0.1% per MeV, from the usual Fermi theory.⁶

Figure 1 illustrates a partial energy level scheme of C^{12} and the beta decay of B^{12} and N^{12} with the measured branches to the levels of C^{12} . Uncertainties in these branches will contribute to uncertainties in the measured shapes of the ground-state transition spectra. The branches to the 4.43-MeV level of C^{12} have been measured by coincidence methods,⁷ and the B^{12} branches to the 7.6-MeV⁸ and 10.1-MeV⁹ levels have been measured by absolute counting of the number of alpha particles emitted following beta decay to these levels.

Mayer-Kuckuk and Michel⁶ have measured the shapes of the two spectra separately over the energy range 5 to 10.5 MeV for B^{12} and 5 to 13 MeV for N^{12} , using an iron-free single-lens magnetic spectrometer. They reported a value for $A + \delta A$ of $1.30 \pm 0.31\%$ per MeV with an energy dependence of $1.82 \pm 0.09\%$ per MeV for B^{12} and $0.60 \pm 0.3\%$ per MeV for N^{12} . They determined the N^{12} branch to the 7.6-MeV level of C^{12} to be $3.0 \pm 0.5\%$ from the shape of the N^{12} spectrum, allowing for a constant shape factor.

Other experiments on beta-alpha¹⁰ and beta-gamma¹¹ angular correlations have been reported which appear to indicate the presence of effects as predicted by the

⁵ A. Schwarzschild, *Bull. Am. Phys. Soc.* **4**, 79 (1959).

⁶ T. Mayer-Kuckuk and F. C. Michel, *Phys. Rev.* **127**, 545 (1962).

⁷ N. W. Glass, R. W. Peterson, and R. K. Smith, *Bull. Am. Phys. Soc.* **6**, 49 (1961). R. W. Peterson and N. W. Glass, preceding paper [*Phys. Rev.* **129**, 292 (1963)].

⁸ C. W. Cook, W. A. Fowler, C. C. Lauritsen, and T. Lauritsen, *Phys. Rev.* **107**, 508 (1957).

⁹ C. W. Cook, W. A. Fowler, C. C. Lauritsen, and T. Lauritsen, *Phys. Rev.* **111**, 567 (1958).

¹⁰ M. E. Nordberg, F. B. Morinigo, and C. A. Barnes, *Phys. Rev.* **125**, 321 (1962).

¹¹ F. Boehm, V. Soergel, and B. Stech, *Phys. Rev. Letters* **1**, 77 (1958).

* Work performed under the auspices of the U. S. Atomic Energy Commission.

¹ R. P. Feynman and M. Gell-Mann, *Phys. Rev.* **109**, 193 (1958).

² M. Gell-Mann, *Phys. Rev.* **111**, 362 (1958).

³ E. Hayward and E. G. Fuller, *Phys. Rev.* **106**, 991 (1957); E. L. Garwin, *ibid.* **114**, 143 (1959); W. C. Barber, F. Berthold, G. Fricke, and F. E. Gudden, *ibid.* **120**, 2081 (1960); S. S. Hanna and R. E. Segel, *Proc. Roy. Soc. (London)* **A259**, 267 (1960).

⁴ M. Gell-Mann and S. M. Berman, *Phys. Rev. Letters* **3**, 99 (1959).

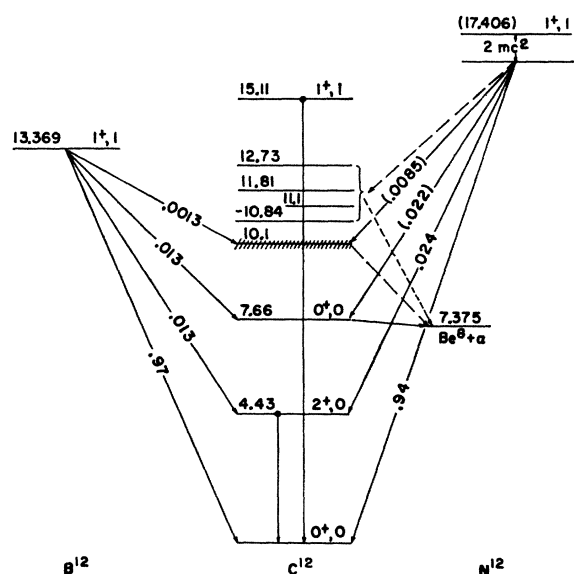


FIG. 1. A partial energy-level diagram of C^{12} showing the principal features of the B^{12} electron and N^{12} positron decays. The numbers in parentheses are results of this experiment. The B^{12} and N^{12} half-lives are 20.2 and 11.0 msec, respectively.

CVCT.^{12,13} For theoretical reasons, however, the measurement of the comparative shapes of the B^{12} and N^{12} beta spectra appears to offer the most clear-cut and least ambiguous¹⁴ means of determining the validity of the CVCT.

In the experiment reported here, a direct comparison of the B^{12} and N^{12} beta spectra is made at corresponding points below the end points, rather than at points of equal energy. No attempt was made to determine the absolute shapes of the spectra individually. A rather different experimental method from that used by Mayer-Kuckuk and Michel is employed in this work.

II. EXPERIMENTAL APPARATUS

A schematic illustration of the specially designed 180° flat field magnetic spectrometer is shown in Fig. 2. Each channel consisted of three plastic fluors, 2×2×10, 2×4×10, and 10×10×10 mm, respectively. The first and second fluors were coupled by means of prisms and quartz light pipes to the photocathodes of photomultiplier tubes, and the third fluor was coupled directly to a corresponding photomultiplier tube by a quartz light pipe. A total of twelve RCA-7265 photomultiplier tubes housed in a magnetically shielded box were used. A triple coincidence was required for a count in each channel. The channels were fixed at radii of 7, 8.33, 9.67, 11, and 12 cm. The magnetic field of the spectrometer was measured and controlled by a Varian

F-8 nuclear magnetic resonance fluxmeter which fed a regulating signal to the magnet power supply.¹⁵

B^{12} was produced via the $B^{11}(d,p)B^{12}$ reaction using 2.0-MeV deuterons, and N^{12} was produced via the $B^{10}(He^3,n)N^{12}$ reaction using 5.25-MeV He^3 particles. The particles were accelerated by the large Los Alamos Van de Graaff machine. The particle beams, after passing through the energy analyzing magnet, were focused to a horizontal line by a single section electrostatic quadrupole lens. After passing through the lens, the beam was deflected a few degrees by an electrostatic deflector and then bent back onto the target in the spectrometer by a trimmer magnet ahead of the spectrometer magnet. This was done to compensate for the deflection of the beam due to the spectrometer magnetic field, and to bring the deuteron and He^3 beams onto the target normally. Since the spectrometer field was reversed to analyze the negative beta particles from B^{12} and the positrons from N^{12} , the deflector and trimmer magnet fields were also reversed. The same thick target was used for both reactions and consisted of a 96% B^{10} -4% B^{11} powder pressed onto the end surface of the Cu target holder. The beam was chopped by a square voltage pulse applied to a deflector at the exit of the beam analyzing magnet. A beam on time of 10 msec and beam off time of 15 msec was generally used. The photomultipliers and counting equipment were gated off during the bombardment period.

The magnet pole pieces were 16 in. in diameter with a 2½-in. gap. Since a direct comparison of the electron spectrum from B^{12} and the positron spectrum from N^{12} was made, it was important that any inhomogeneities in the magnetic field reproduce themselves when the field was reversed to analyze the opposite polarity particles. The absolute homogeneity of the field was of secondary importance. The fractional variation of the fields along

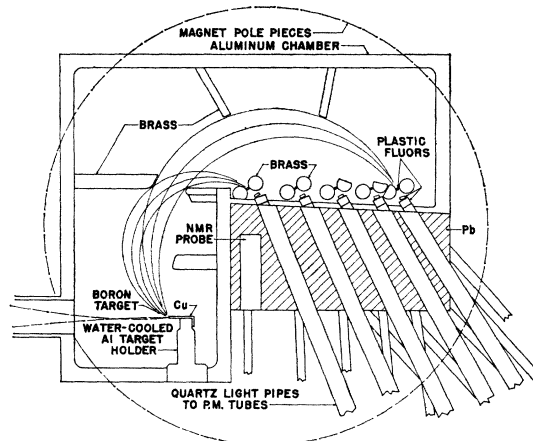


FIG. 2. Five-channel beta-ray spectrometer. Channels are at radii of 7.0, 8.33, 9.67, 11, and 12 cm. Magnet pole pieces are 16 in. in diameter with 2½-in. gap. Light pipes are 3 ft long.

¹² J. Bernstein and R. Lewis, Phys. Rev. **112**, 232 (1958).

¹³ H. A. Weidenmüller, Phys. Rev. Letters **4**, 299 (1960).

¹⁴ H. A. Weidenmüller, Nucl. Phys. **21**, 397 (1960).

¹⁵ The power supply was designed and built by W. P. Aiello of this laboratory.

orthogonal axes was measured for the two polarities with field strengths in the ratio of the N¹² positron end-point momentum and B¹² electron end-point momentum. The maximum difference in the variations of the fields for opposite polarities was less than two parts in 10⁴ over the area used in the spectrometer.

To prevent gain changes from stray magnetic fields on the photomultiplier tubes as the magnetic field was reversed, it was necessary to magnetically shield the tubes. The tubes were housed in an iron box with each tube separately enclosed in a mu-metal shield. An additional shielding apron was mounted on the box to bypass the stray fields. Gain changes caused by reversing the field were less than two percent.

The light collection efficiency through the 3-ft-long quartz light pipes was low, particularly from the small fluors; hence, high-gain low-noise-level photomultiplier tubes were used. Typical pulse-height distributions from the beta particles passing through the fluors are shown in Fig. 3. Although the distributions are broad, the coincidence counting rates were quite insensitive to changes in gain with the low bias settings used. In practice, the gains were set by increasing the gain of each photomultiplier-amplifier combination until a coincidence counting rate plateau was reached. The criterion usually used was that a factor of two change in gain in either direction cause less than 10% change in coincidence counting rate. The amplifiers were three-stage negative feed-back type, with a rise time of 6×10^{-8} sec, designed by R. D. Hiebert of this laboratory.

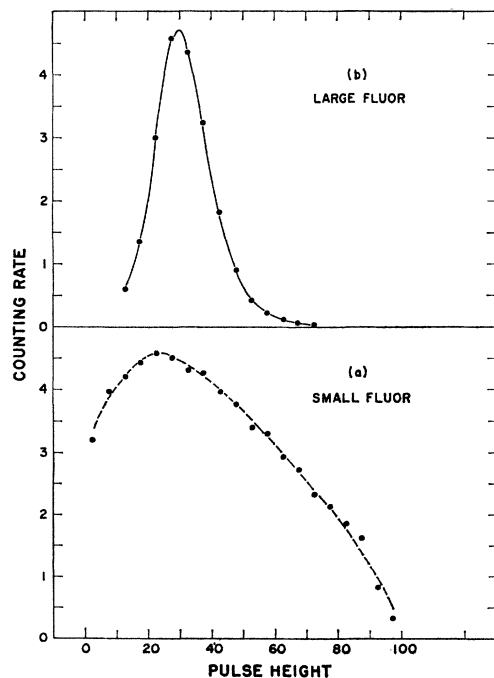


FIG. 3. (a) Typical coincidence pulse-height distribution from first small fluor in each channel; (b) Distribution from larger third fluor.

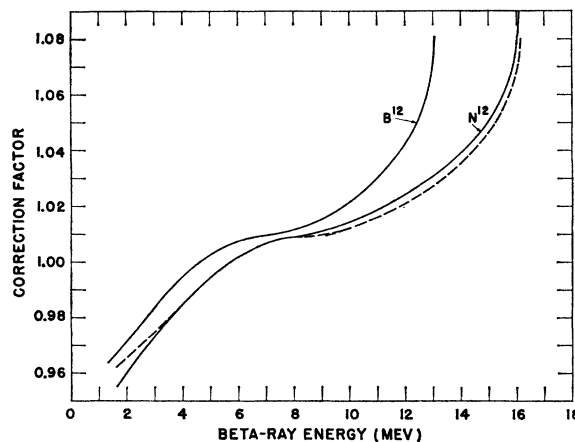


FIG. 4. Inner bremsstrahlung correction factors to be applied to measured spectra as calculated by Schwarzschild (reference 5). Dashed line is B¹² correction when B¹² end point is normalized to the N¹² end point.

III. EXPERIMENTAL METHOD

The Fermi momentum spectrum for an allowed beta transition is given by

$$N(p)dp = CF(Z,E)p^2[(1+p_0^2)^{1/2} - (1+p^2)^{1/2}]^2 dp, \quad (2)$$

The factor $F(Z,E)$ for $Z=6$ and $E>2$ MeV is constant to a small fraction of a percent for both electron and positron decay, and the factor $p^2[(1+p_0^2)^{1/2} - (1+p^2)^{1/2}]^2$ can be approximated by $p^2(p_0-p)^2$ to less than one percent error for $p_0=27.14mc$ (B¹²) and $p>4mc$. Furthermore, $p^2(p_0-p)^2$ (N¹²)/ $p^2(p_0-p)^2$ (B¹²) approximates the more exact ratio to less than 0.3% for $p/p_0>0.15$. Therefore, the Fermi ground state momentum spectral shapes for N¹² and B¹² are the same to a negligible difference above 2 MeV (B¹²) when normalized to the end-point momenta. A direct comparison of the spectral shapes normalized to the end points will then, in principle, give a measurement of the comparative deviation from allowed Fermi spectra when corrected for branches to higher levels. Possible corrections due to inner bremsstrahlung effects must also be considered. Figure 4 illustrates calculated⁵ correction factors to be applied to B¹² and N¹² spectral measurements to account for the inner bremsstrahlung effects. The dashed curve is the B¹² correction when the B¹² end point is normalized to the N¹² end point. Thus, the correction required for a direct comparison is small.

The measured relative spectral shapes near the end points depend critically upon the proper normalizing of the end points in the spectrometer. The B¹² and N¹² end points were set as nearly as possible to the same position in the spectrometer by equalizing the ratios of the counts obtained in the two high-energy channels for the two spectra. Nominal end-point settings of 12.5- and 13.0-cm radii were used for this purpose. The relative end-point momenta of the spectra can then be obtained from the ratio of magnetic field strengths required to equalize the ratios of counts.

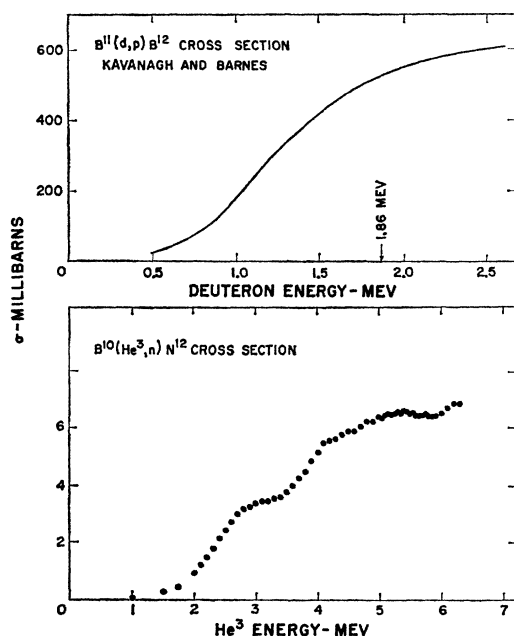


FIG. 5. Activation cross sections for $B^{11}(d,p)B^{12}$ and $B^{10}(He^3,n)N^{12}$ reactions. The plots are normalized at 5.0-MeV He^3 energy and 1.86-MeV deuteron energy. At these energies the He^3 and deuteron ranges in boron are nearly the same.

The effect of relative errors in setting the end points can be seen from

$$\frac{\Delta R}{R} = \Delta \left[\frac{\rho_1^2(\rho_0 - \rho_1)^2}{\rho_2^2(\rho_0 - \rho_2)^2} \right] / \left[\frac{\rho_1^2(\rho_0 - \rho_1)^2}{\rho_2^2(\rho_0 - \rho_2)^2} \right] = \frac{2(\rho_1 - \rho_2)\Delta\rho_0}{(\rho_0 - \rho_1)(\rho_0 - \rho_2)}, \quad (3)$$

where R is the ratio of counts obtained in any two channels at radii ρ_1 , ρ_2 ; and ρ_0 is the end-point radius in the spectrometer.

A possible source of differential distortion in the comparison of the spectra may arise from the use of the thick boron target, if the source distributions as a function of depth in the target are appreciably different for B^{12} and N^{12} . A comparison of the activation cross sections as a function of energy for the $B^{11}(d,p)B^{12}$ and $B^{10}(He^3,n)N^{12}$ reactions^{16,17} is shown in Fig. 5. The range of 5.0-MeV He^3 particles in boron is 5.5 mg/cm² which is nearly the same as the range of 1.9-MeV deuterons. The gross shapes of the two activation curves are comparable when normalized at these energies as is shown in the figure. The use of a thick target with these incident particle energies would then appear to give a negligible distortion of relative shapes of the spectra, since the total active source depth is small for high-

energy beta particles. In this experiment, 2.0-MeV deuterons and 5.25-MeV He^3 particles were used.

In practice, beam currents of $\sim 10 \mu A$ of He^3 particles and $\sim 2 \mu A$ of deuterons on the target were used. At these beam intensities the background and accidental coincidence rate was less than one percent of the true count rate in each channel over most of the spectrum. On some runs the deuteron current was varied over a wide range to check on the accuracy of background and accidental coincidence corrections, and also to check for possible dead time effects.

Many runs were taken under various conditions of chamber baffling, magnetic shielding on the photomultiplier tubes, electronic arrangements, and gain settings. The results were, in general, insensitive to these changes, although in some cases the point-scatter was worse than others.

Electron and Positron Scattering

It is well established that electrons and positrons scatter differently while passing through material.¹⁸ For single scattering off nuclei of low Z and electron energies above 1 MeV the differential scattering cross section is given by

$$\sigma = \sigma_R \{ [1 - \beta^2 \sin^2(\Theta/2)] + (\pi Z\beta/137) \sin(\Theta/2) [1 - \sin(\Theta/2)] \}, \quad (4)$$

where $\sigma_R = (Z^2/2pv)^2 \csc^4(\Theta/2)$ is the Rutherford cross section. For positron scattering, Z is replaced by $-Z$. Hence, positrons scatter less than electrons at high angles. This effect shows up in the ratio of electron to positron backscattering coefficients. This ratio is 1.3, independent of Z .¹⁹

The effects of scattering differences for electrons and positrons as a function of energy on the channel counting efficiencies were studied to determine if corrections to the data were necessary. Some beta particles will scatter out of the first fluor and not transverse the second and third fluors. In general, the fraction scattering out will increase with decreasing energy. It is necessary, then, to determine if the differing energy of the electrons and positrons in each channel, as well as differences due to electron and positron scattering, will cause a distortion in the direct comparison.

The first fluor is 0.2 g/cm² thick and the composition is effectively CH. The carbon is the main contributor to the scattering.

An auxiliary experiment was performed to measure the electron and positron scattering in fluor material as a function of energy. A schematic diagram of the apparatus is shown in Fig. 6. Electrons from the decay of B^{12} and positrons from the decay of N^{12} were used for the measurement. A triple coincidence between the three fluors was required for a count and, in addition, the

¹⁶ R. W. Kavanagh and C. A. Barnes, Phys. Rev. **112**, 503 (1958).

¹⁷ R. W. Peterson and N. W. Glass, preceding paper [Phys. Rev. **129**, 292 (1963)].

¹⁸ H. Feshbach, Phys. Rev. **88**, 295 (1952).

¹⁹ *Beta- and Gamma-Ray Spectroscopy*, edited by K. Siebahn (North-Holland Publishing Company, Amsterdam, 1955), p. 8.

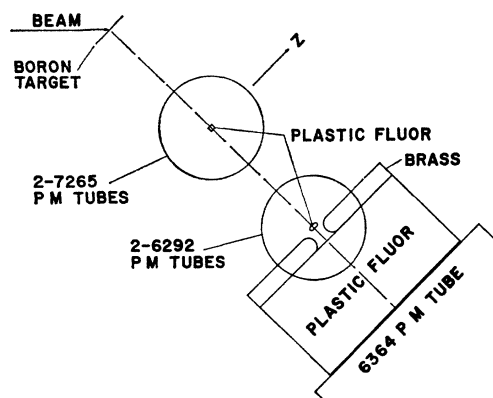


FIG. 6. Schematic diagram of apparatus used to measure multiple scattering angular distributions of electrons and positrons from fluoro material.

coincidence pulse-height distribution from the third large fluoro was recorded on a 100-channel pulse-height analyzer. The angular distribution was measured by displacing the first fluoro and photomultipliers in the Z direction. The counts obtained in each position were normalized by means of a beam current integrator. The measurement yielded angular distributions as a function of energy of scattered beta particles. These distributions were compared with Molière's multiple scattering theory²⁰ to determine mean scattering angles as a function of energy. The results are shown in Fig. 7 for a scattering fluoro $3 \times 3 \text{ mm} \times 2\frac{1}{2} \text{ cm}$. The solid line shows the calculated mean scattering angles from a 2-mm \times 2-mm fluoro of effective composition CH using Molière's electron multiple scattering theory.

The channel efficiencies for electrons were estimated by using the calculated mean scattering angles and distributions. For positrons, the efficiencies were estimated using mean scattering angles obtained by multiplying the calculated electron mean scattering angles by the experimental ratio of positron to electron mean scattering angles at each energy.

IV. DATA AND CORRECTIONS

Basic Data

Figure 8(a) shows the basic data obtained for a series of normalized magnet field settings. The data are plotted as N¹² counts in each channel divided by the corresponding B¹² counts normalized to unity at the 9.67-cm channel except for the 12.5-cm end-point data which are displaced for plot clarity. The ratio of magnetic fields for the N¹² measurements to the magnetic fields for the B¹² measurements was 1.2167.

Initially, the spectrometer was set up without the cylindrical brass slits ahead of each channel and runs were taken. Accidental coincidence corrections were

²⁰ G. Molière, *Z. Naturforsch.* **3a**, 78 (1948). See also reference 19, p. 4.

larger, since there were more true second and third fluoro coincidences in accidental coincidence with noise and background pulses from the first fluoro detector system for each channel. The points from this series of runs scatter more than with the later geometry. Figure 8(b) shows the data obtained under these conditions.

Corrections

The data shown in Fig. 8 are uncorrected except for the small background and accidental coincidence subtractions. Additional corrections considered are as follows:

- (1) channel efficiencies as a function of energy and particle type,
- (2) annihilation loss of positrons before detection in all three fluoros of each channel,
- (3) differences in backscattering of electrons and positrons from the source and holder,
- (4) differences in inner bremsstrahlung effects,
- (5) branching to the 4.43-MeV level in C¹²,
- (6) possible effects due to higher order terms independent of the CVCT,
- (7) errors in setting the end points to the same position in the spectrometer.

These corrections are listed in Table I with their effect and estimated uncertainties on the comparative slope between 8.0 and 14.4 MeV (N¹² scale). Corrections (1), (4), and (7) were discussed in the preceding section.

Correction (2) was calculated²¹ from

$$\Phi(E)dE = NZ\rho^{-1}\phi(E)(dE/dx)^{-1}dE, \quad (5)$$

where $\Phi(E)$ is the probability per unit energy of a positron of kinetic energy E annihilating in a material of density ρ and stopping power dE/dx . $\phi(E)$ is the annihilation cross section given by Heitler.²² An average energy loss of 1.5 MeV before detection was assumed with a 50% uncertainty.

TABLE I. Corrections applied to the data and their effects and uncertainties on the experimental value of $A + \delta A$ between 8 and 14.4 MeV (N¹² scale).

Correction	Effect (%/MeV)	Uncertainty (std. dev.) (%/MeV)
(1) Channel efficiencies	-0.25	±0.12
(2) Annihilation loss	+0.09	±0.05
(3) Backscattering	+0.14	±0.14
(4) Inner bremsstrahlung	-0.06	±0.02
(5) 4.43 level branches	-0.24	±0.03
(6) Higher order terms	-0.12	±0.06
(7) End-point errors	...	±0.17
Least-squares fits	...	±0.10
Total	-0.44	±0.28

²¹ H. Hilton, Ph.D. thesis, California Institute of Technology, 1960 (unpublished).

²² W. Heitler, *The Quantum Theory of Radiation* (Clarendon Press, Oxford, 1954), 3rd ed., p. 268.

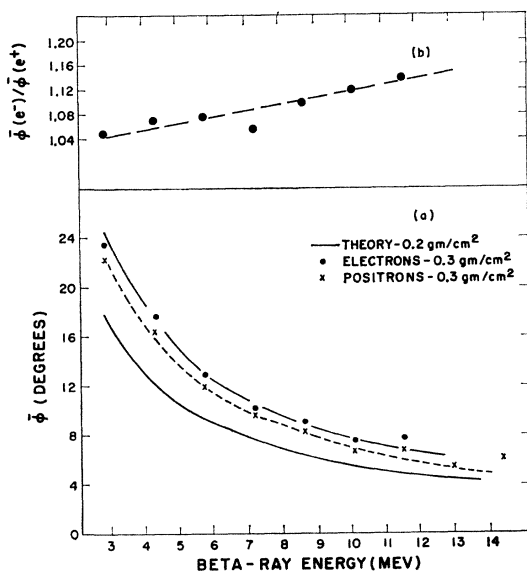


FIG. 7. (a) Results of auxiliary experiment on electron and positron scattering from 0.3 g/cm² of fluor material. $\bar{\phi}$ is mean multiple scattering angle. Solid line is calculated by Molière's electron multiple scattering theory for 0.2 g/cm² of fluor material. (b) Measured ratios of electron to positron mean scattering angles.

Effect (3) was aggravated somewhat by the use of a Cu target holder which was used because of the high beam currents. The correction was calculated by folding the backscattered electron energy distribution as given by Bothe²³ with the Fermi spectrum. Ten percent of the electrons and 10/1.3% of the positrons through the defining baffle were assumed to be backscattered. The correction tends to increase the slope and is assigned a 100% uncertainty.

Correction (5) is straightforward. The measured⁷ branching ratios and uncertainties of $1.3 \pm 0.1\%$ for B¹² decay, and $2.4 \pm 0.2\%$ for N¹² decay to the 4.43-MeV C¹² level were used.

If the energy-dependent terms in the two spectra are linear, and equal and opposite in sign, there is an exact correspondence between the experimental slope and $A + \delta A$. On the other hand, it is possible there are appreciable linear and/or nonlinear energy-dependent terms of the same sign in the two spectra. These will affect the experimental value of $A + \delta A$ because a larger energy interval was taken for N¹² than for B¹². Morita's²⁴ estimates of non-CVCT higher order terms were used for calculating this correction. An uncertainty of 50% is assigned to this correction which tends to decrease the slope.

A small correction due to effect (7) was applied to the data. The ratio of magnetic fields for the N¹² measurements to the magnetic fields for the B¹² measurements was 1.2167. An adjustment corresponding to a shift of +0.0008 in this ratio was applied. Assuming a

²³ W. Bothe, Z. Naturforsch. 4a, 542 (1949). See also reference 19, p. 8.

²⁴ M. Morita, Phys. Rev. 113, 1584 (1959).

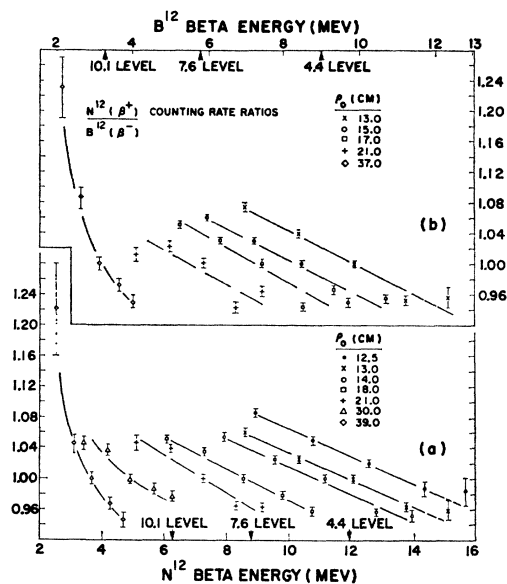


FIG. 8. (a) Measured N¹²/B¹² ratios at seven different end-point radii with chamber geometry as shown in Fig. 2. Arrows indicate branching end points. (b) Data taken before cylindrical brass slits ahead of each channel were installed.

constant value for $A + \delta A$, then the measured ratio of N¹² end-point momentum to B¹² end-point momentum becomes 1.2175 ± 0.0011 . Taking 13.369 ± 0.001 MeV as the B¹² ground-state transition energy²⁵ and using this momentum ratio, the N¹² positron spectrum to the ground state has an end-point energy of 16.384 ± 0.015 MeV. The value from reaction data is given as 16.43 ± 0.06 MeV.²⁵

V. RESULTS

The experimental points of Fig. 8(a) after corrections (1) through (7) have been applied are shown in Fig. 9.

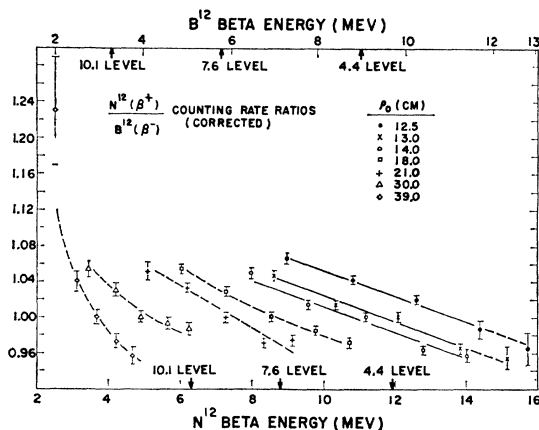


FIG. 9. Data of Fig. 8(a) after corrections have been applied. Solid lines are least-squares fits. Statistical errors only are shown.

²⁵ Landolt-Börnstein Tables, edited by K. Hellwege (Springer-Verlag, Berlin, 1961), New Series, Gp. I, Vol. 1.

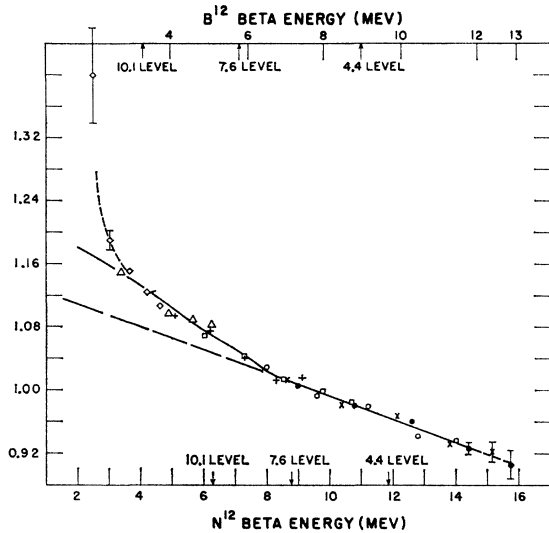


Fig. 10. Composite plot of N¹²/B¹² ratios shown in Fig. 9.

Linear least-squares fits are shown for the 12.5-, 13-, and 14-cm end-point data. These give values for $A + \delta A$ of 1.60 ± 0.11 , 1.64 ± 0.19 , and $1.63 \pm 0.17\%$ per MeV, respectively, where the average B¹², N¹² energy interval is used. The average of these three values is $1.62 \pm 0.10\%$ per MeV. After applying the estimated uncertainties in the corrections as listed in Table I, the error is increased to $\pm 0.28\%$ per MeV.

The final value from the experiment is, thus,

$$A + \delta A = 1.62 \pm 0.28\% \text{ per MeV} \quad (6)$$

measured from 8 to 14.4 MeV on the N¹² positron spectrum, and from 6.5 to 11.7 MeV on the B¹² electron spectrum. This value is to be compared with the predicted value of $1.10 \pm 0.17\%$ per MeV⁶ on the basis of the conserved vector current theory, and approximately 0.10% per MeV from the usual Fermi theory. Hence, this result appears to definitely show the existence of such an effect as predicted by the CVCT but somewhat larger than predicted. Mayer-Kuckuk and Michel⁶ obtained $1.30 \pm 0.31\%$ per MeV from their experiment which overlaps the predicted value, but, on the other hand, is not in serious disagreement with the value reported here.

The 18-, 21-, 30-, and 39-cm end-point data were analyzed in order to determine branching ratios for N¹² decay to higher levels in C¹². The results of this analysis depend partially upon previously measured B¹² branching ratios. A ratio of $1.3 \pm 0.4\%$ ⁸ for the B¹² beta decay branch to the 7.66-MeV level of C¹², and $0.13 \pm 0.04\%$ ⁹ for the branch to the 10.1-MeV level were used. A constant value of $A + \delta A = 1.62 \pm 0.28$ was assumed over the measured spectra. The results are $2.2 \pm 0.6\%$ for the N¹² branching ratio to the C¹² 7.66-MeV level and $0.85 \pm 0.6\%$ for the branching ratio to the 10.1-MeV level.

A composite plot of the data shown in Fig. 9 is illustrated in Fig. 10. The solid lined curve was constructed from the central values of the slope and various branching ratios given above. A consistent picture is thus presented with the exception of the two or three data points at lowest energy. This deviation of the data at the extreme low-energy end of the measured spectra, if taken seriously, can be accounted for by assuming a N¹² decay branch of the order of $\frac{1}{2}\%$ to one or more levels at ~ 12 MeV.

VI. CONCLUSION

In summary, the results of this experiment are:

- (1) a value for $A + \delta A$ of $1.62 \pm 0.28\%$ per MeV;
- (2) an end-point energy of 16.384 ± 0.015 MeV for the N¹² positron spectrum to the ground state of C¹²;
- (3) $2.2 \pm 0.6\%$ for the N¹² positron decay branching ratio to the 7.66-MeV level of C¹², $0.85 \pm 0.6\%$ for the N¹² branching ratio to the 10.1-MeV level of C¹², and an indication of a branch of the order of $\frac{1}{2}\%$ to one or more C¹² levels around 12 MeV.

Aside from the always present possibility of undetected systematic errors in an experiment of this nature, the value for $A + \delta A$ is larger than the theoretically predicted value of $1.10 \pm 0.17\%$ per MeV on the basis of the CVCT, but seems to definitely indicate the presence of some such effect. The disagreement with the experimental value of $1.30 \pm 0.31\%$ per MeV by Mayer-Kuckuk and Michel⁶ is not so serious, and to some extent hinges on the value of the N¹² branching ratio to the C¹² 7.66-MeV level. *Note added in proof.* Y. K. Lee, L. W. Mo, and C. S. Wu have recently repeated the measurement of the individual shape factors for B¹² and N¹². They used an intermediate image lens spectrometer and obtained an energy dependence of $+0.57 \pm 0.11\%$ per MeV for B¹² and $-0.62 \pm 0.06\%$ per MeV for N¹², with an additional uncertainty of 0.2% per MeV for N¹² due to the end-point uncertainty. Their value for $A + \delta A$ is thus $1.19 \pm 0.24\%$ per MeV. [Invited paper by C. S. Wu, Bull. Am. Phys. Soc. 8, 71 (1963); and C. S. Wu (private communication).]

As pure speculation, there may be the possibility that an anomalously high value for $A + \delta A$ is connected in some way with what appears to be a real difference in the B¹² and N¹² beta-decay ft values for the ground-state transitions.⁷

ACKNOWLEDGMENTS

We wish to acknowledge and thank the many people whose help and support made this work possible. Particular thanks are due J. L. McKibben and members of the Van de Graaff accelerator group for their cooperation and active support. Dan L. Davis, a graduate summer student, assisted materially on some phases of the work.